J Nanostruct 16(1): 394-399, Winter 2026

RESEARCH PAPER

Fe_2O_3 Nanoparticles Synthesis and Characterization

Masar Alaa Abdulkhaleq *, Nadia Abdulkarim Abdulrahman

Department of Chemistry, College of Science, University of Baghdad, Baghdad, Iraq

ARTICLE INFO

Article History:
Received 15 September 2025
Accepted 23 October 2025
Published 01 January 2026

Keywords:
Fe_2O_3
Hydrothermal
Iron (III) oxide
Nanoparticles

ABSTRACT

In this work iron (III) oxide (Fe_2O_3 In this work hydrothermal method was used for synthesize iron (III) oxide nanoparticles at several temperatures. Ferric chloride hexahydrate ($FeCl_3.6H_2O$) was used for the preparation, the preparation was carried out at pH 9 and 60, 100 and 160 °C. Size, structure and optical band gab were determined by using UV-Vis (Ultraviolet Visible) analysis, XRD (X ray diffraction) and SEM (Scanning Electron Microscope). Hematite (the other name for Fe_2O_3) that prepared by hydrothermal method has small size and good crystallinity. UV-Vis spectroscopy showed a red shift for the absorption peak at 160 °C. the average diameters of the nanoparticles decreased with a comparable rise in temperature, according to FE-SEM microscopy. XRD crystallography showed a good structural pattern for Fe_2O_3 nanoparticles with a decrease in crystallite size as temperature increased. In addition, XRD results data exhibit a rhombohedral (hexagonal) structure and revealed an average size of 23, 12, 11.7nm at temperatures range of: 60,100 and160 °C, respectively, which is consistent with SEM images. Hematite prepared by 160 °C has lower average size, better crystallinity, highest band gap compared to the hematite prepared by 60 and 100 °C.

How to cite this article
Abdulkhaleq M., Abdulrahman N. Fe_2O_3 Nanoparticles Synthesis and Characterization. J Nanostruct, 2026; 16(1):394-399. DOI: 10.22052/JNS.2026.01.035

INTRODUCTION

A promising and rapidly expanding field of study, nanotechnology has achieved great success in the age of contemporary technology. Materials with distinctive size (often falling between 1 and 100 nm), structure, electric, magnetic, mechanical physio-chemical, thermal, catalytic, optical scattering and form characteristics are called nanoparticles [1]. The ultra-small size and large surface area is largely determining the properties and reactivity of the nanoparticles [2]. The smaller sizes magnetic nanoparticles which are less than 100 nm and narrow particle size distribution with high magnetization values are essentially required for applications Reduction in size results in notable effects on the magnetic ordering within the particles because the surface layer's magnetic structure is different from the particle core's [3]. Hematite, maghemite, and magnetite are the three major types of iron oxides, which are extremely significant minerals. Hematite (Fe_2O_3) is the more stable of them under ambient conditions and also the more ecologically friendly and semiconductor (e.g., 2.1 eV) [4]. Hematite (Fe_2O_3) is more stable with anti-corrosive abilities, tunable optical and magnetic properties, high chemical stability and biological compatibility with inexpensiveness that suitable for a wide range of technological

* *Corresponding Author Email: massar.alaa1605a@sc.uobaghdad.edu.iq*

applications. These benefits of hematite allowed for development of creative nano technologies for applications in catalysts, anticorrosive agents high-density magnetic storage media, pigments, water splitting, water purification, solar energy conversion and gas sensors [5]. Iron oxide nanoparticles have been synthesized by using the hydrothermal process [6], co-precipitation [7], micro emulsion, thermal decomposition [8], sol-gel processing, and other methods. Therefore, the preparations and applications of iron oxide nanoparticles have attracted more and more researchers [9].

Hydrothermal synthesis of nanoparticles is more preferable because it can be appropriately expanded for large-scale nanoparticle synthesis [10]. Hydrothermal synthesis would be more commercially viable if the nanoparticles could be synthesized more faster in the reaction containers. One of the most used techniques for producing nanoparticles under high pressure and temperature is hydrothermal synthesis [11]. The ease of large-scale manufacture, high-crystallized powders with narrow particle size distribution, excellent purity, and adjustable process parameters like solute concentration are some advantages of the hydrothermal synthesis approach [12]. There are two primary components to a hydrothermal system: i) The unit that controls temperature. ii)The reactor; which consists of Teflon lined stainless steel autoclaves.

In this work, we aimed to investigate the effect of temperature change for synthesis of iron oxide at the shape, optical band gap, size and morphology of the particles. We used hydrothermal technique to synthesize pure Fe_2O_3 nanoparticles. Their optical, morphological and structural properties were ascertained using characterization methods such as the UV-Vis (Ultraviolet-visible analysis), SEM (Scanning Electron Microscopy) and XRD (X-ray diffraction).

MATERIALS AND METHODS

Materials

Ferric chloride hexahydrate ($FeCl_3.6H_2O$), Ammonium hydroxide (NH_4OH), distilled water and ethanol.

Methods

Hydrothermal method was used to prepare iron oxide nanoparticle (Fe_2O_3 NPs). Firstly, 50ml of distilled water was used to dissolve 2g of $FeCl_3.6H_2O$ before heating at 80 °C for 30 min with magnetic stirring. To maintain the pH value to 9.2, 25ml of 2M ammonium hydroxide was added. Then, the solution was hydrothermally treated after transferred it into the reactor (Teflon-lined stainless-steel autoclave) for several temperatures of (60,100,160) °C for 8 hours. Centrifugation was used for 5 minutes at 3500 rpm in order to separate the yield and after that washed for several times with distilled water and ethanol, and finally, the yield was dried in air for 1 hour at 80 °C and calcined for 4 hours at 700 °C.

RESULTS AND DISCUSSION

UV-Visible Analysis

The UV-Vis absorption spectra of the three

Fig. 1. Hydrothermal system. a) Temperature control unit b) The Reactor which consists of Teflon lined autoclave.

samples hydrothermally produced of iron (III) oxide nanoparticles at varying temperatures showed that all absorption UV-Vis curves indicate a highly absorption between 550and 650 nm wavelength. UV-Vis spectra showed absorption peaks at 573, 610 and 568 nm for Fe_2O_3 NPs synthesized at three different temperatures of 60,100, and 160 °C, respectively (Fig. 3). The absorption results are in compatible with data from other studies [13]. The band gap energy E_g values can be calculated. by applying the following Eq. 1 [14]:

$$E_g = h\,C / \lambda \quad (1)$$

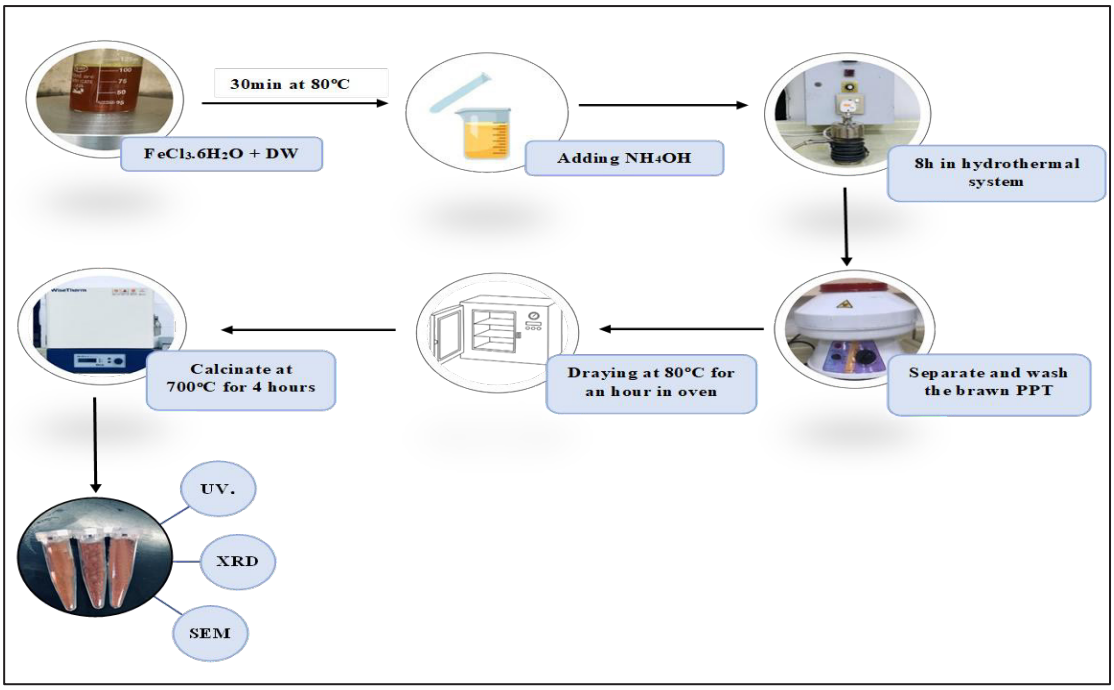

Fig. 2. Flowchart for the synthesis of iron oxide (Fe_2O_3) nanoparticles by hydrothermal method.

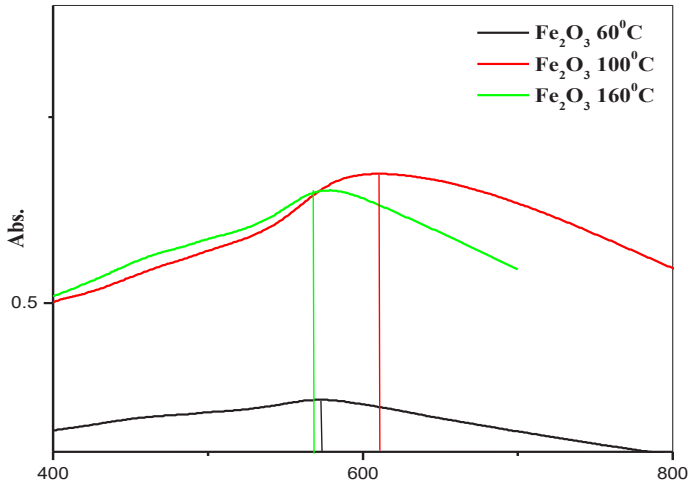

Fig. 3. UV-Vis spectra at the region of 400-800 nm for Fe_2O_3 NPs prepared at several temperatures of 60, 100 and 160 °C.

Where h is the Plank constant = ($4.135667x10^{-15}$eV.s), C is the speed of light in vacuum = ($3.00x10^8$ m/s), and λ is the maximum wavelength of the absorption peaks in nm (λ_{max}).

Maximum wavelength of the absorption peak is 573nm at a temperature of 60 °C, the value of E_g was found to be 2.16. At 100 °C, λ_{max} of the absorption peak was 610nm and the value of E_g was 2.03. While for 160 °C, λ_{max} of the absorption peak is 568nm with 2.18 E_g value. Generally. It was showed that when the wavelength of the absorption UV-Vis peaks reduced, the Eg values increased. The higher band gap energy tends to shift the absorption to higher energies (short wavelength), which means that near states from conduction band are full of electrons and for this reason the electrons will need more energy to transfer, this appears as high Eg value [15].

XRD crystallography

Nature of crystals, crystal size, shape, purity and crystallinity of Fe_2O_3 NPs are given by XRD crystallography. Wurtzite crystallites with hexagonal shape match the structural pattern for pure iron (III) oxide as reported by JCPDS (Joint Committee on Powder Diffraction Standards) card no 33-0664. At various temperatures of 60, 100 and 160 °C, XRD crystallography revealed strong diffraction angles for the indices of 012, 104, 110, 113, 024, 116, 018, 214 and 300 across a range of diffraction angles of 10 to 80 degree (Fig. 4).

The mean crystallite size was calculated by applying Debye–Scherrer Eq. 2:

$$D = K\lambda / \beta \cos\Theta \quad (2)$$

Where D is the crystallite size (nm), k is the Scherrer's constant of value 0.89, λ is the X-ray wavelength (λ=1.54056 Å), β is the full width of the assessment peak at half maximum (in radian) and Θ is Bragg's angle [16]. Thus, at three varying temperatures of 60, 100 and 160 °C the mean crystallite size of Fe_2O_3 NPs was decreased from 27 to 12 to 11.7nm, respectively, which means that Fe_2O_3 NPs that prepared by hydrothermal method is in nanoscale. Additionally, it was discovered that the peak intensities for Fe_2O_3 NPs had decreased, which clearly suggested a decreased in crystallite size.

FE-SEM microscopy

Fig. 5 shows FE-SEM images for Fe_2O_3 NPs

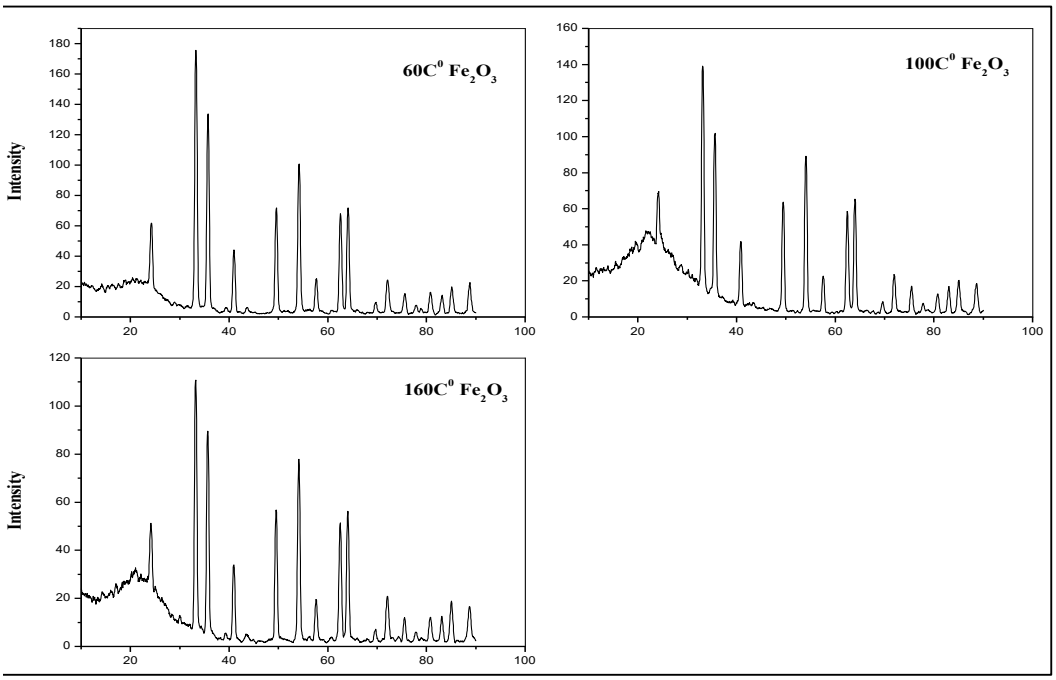

Fig. 4. XRD crystallography for Fe_2O_3 NPs at temperatures of 60, 100 and 160 °C. The patterns exactly match the Reference code number:33-0664 stated pattern, indicating a wurtzite hexagonal structure.

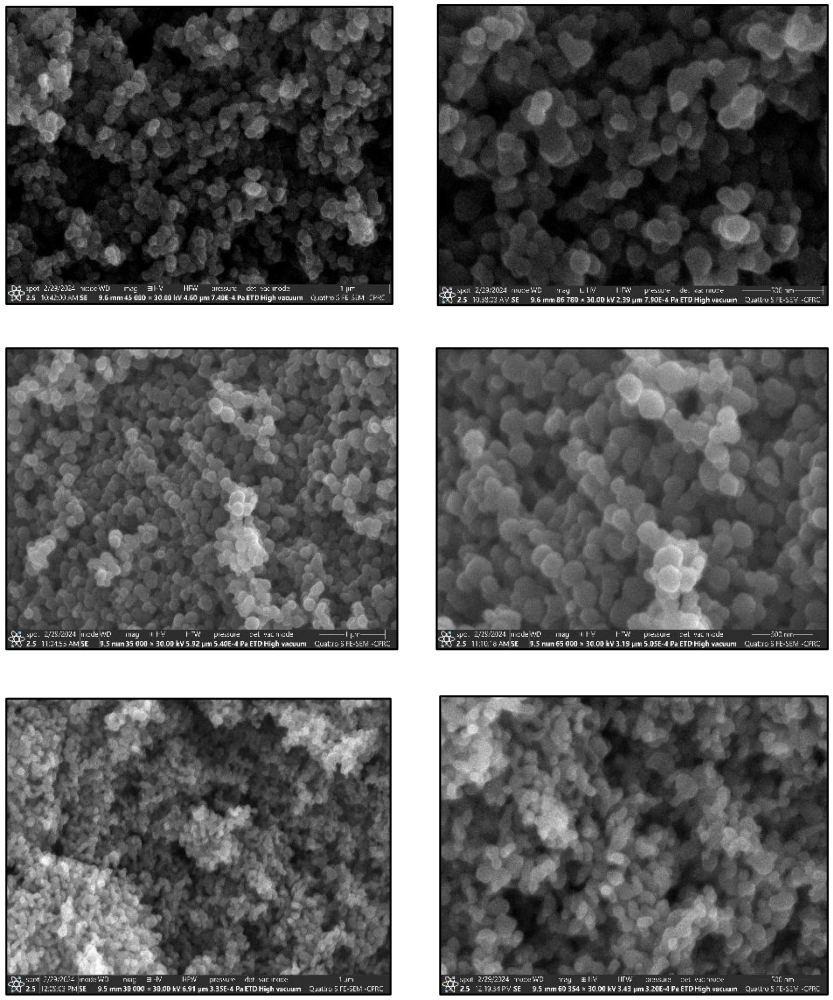

Fig. 5. FE-SEM images for Fe_2O_3 nanoparticles synthesized at 60 °C (a,b), 100 °C (c,d), 160 °C (e,f), utilizing a hydrothermal system with a stainless-steel autoclave lined with Teflon. Images are shown in two scales of 500 nm and 1µm.

synthesized at three different temperatures of 60 °C (a,b), 100 °C (c,d) and 160 °C (e,f) and at two different scales bars of 500nm and 1 µm. Fe_2O_3 NPs synthesized under lower temperature were agglomerated into dots-like shape. While the nanorods' shape is formed at temperature rising (160 °C). In Fig. 5(a, b), it was revealed that Fe_2O_3 NPs had dots-like forms and ranged in size from 100 to 200 nm on average. In Fig. 5(c, d) it was revealed that Fe_2O_3 NPs had dots-like forms and ranged in size from 90 to 200 nm on average. In Fig. 5(e, f), it was revealed that Fe_2O_3 NPs had variation from dots to rod like forms and ranged in size from 60 to 200 nm on an average. The nanocrystals agglomerated as well, which is mainly consist of nanoparticles that agglomerate with each others. These nanoparticles tend to agglomerate because of its high surface energy and high surface stress [17].

CONCLUSION

1. Fe_2O_3 NPs can be synthesized by hydrothermal method using Ferric chloride hexahydrate ($FeCl_3.6H_2O$) at range of temperatures of 60, 100 and 160 °C for 8 hours.
2. In this study all techniques that was used refer to successful synthesis for Fe_2O_3 crystallites with a hexagonal short elongation; which agglomerated into nanoparticles measuring, on average, (23, 12, 11.7) nm in size crystallites with wurtzite-like shapes at 60, 10 and, 160 °C, respectively.

3. XRD Crystallography showed that Fe_2O_3 NPs prepared at 160 °C were smaller than that prepared at 60 and 100 °C.

4.

CONFLICTS OF INTEREST

The authors have no conflicts of interest to declare that are relevant to the content of this article.

REFERENCES

1. Priya, Naveen, Kaur K, Sidhu AK. Green Synthesis: An Eco-friendly Route for the Synthesis of Iron Oxide Nanoparticles. Frontiers in Nanotechnology. 2021;3.
2. Campos EA, Stockler Pinto DVB, Oliveira JISd, Mattos EDC, Dutra RDCL. Synthesis, Characterization and Applications of Iron Oxide Nanoparticles - a Short Review. Journal of Aerospace Technology and Management. 2015;7(3):267-276.
3. Bhavani P, Rajababu CH, Arif MD, Reddy IVS, Reddy NR. Synthesis of high saturation magnetic iron oxide nanomaterials via low temperature hydrothermal method. J Magn Magn Mater. 2017;426:459-466.
4. Wang F, Qin XF, Meng YF, Guo ZL, Yang LX, Ming YF. Hydrothermal synthesis and characterization of α-Fe2O3 nanoparticles. Mater Sci Semicond Process. 2013;16(3):802-806.
5. Pallela PNVK, Ummey S, Ruddaraju LK, Gadi S, Cherukuri CS, Barla S, et al. Antibacterial efficacy of green synthesized α-Fe_2O_3 nanoparticles using Sida cordifolia plant extract. Heliyon. 2019;5(11):e02765.
6. Ozel F, Kockar H, Karaagac O. Growth of Iron Oxide Nanoparticles by Hydrothermal Process: Effect of Reaction Parameters on the Nanoparticle Size. Journal of Superconductivity and Novel Magnetism. 2014;28(3):823-829.
7. Lassoued A, Lassoued MS, Dkhil B, Ammar S, Gadri A. Synthesis, photoluminescence and Magnetic properties of iron oxide (α-Fe2O3) nanoparticles through precipitation or hydrothermal methods. Physica E: Low-dimensional Systems and Nanostructures. 2018;101:212-219.
8. Samrot AV, Sahithya CS, Selvarani A J, Purayil SK, Ponnaiah P. A review on synthesis, characterization and potential biological applications of superparamagnetic iron oxide nanoparticles. Current Research in Green and Sustainable Chemistry. 2021;4:100042.
9. Li Y, Wang Z, Liu R. Superparamagnetic α-Fe_2O_3/Fe_3O_4 Heterogeneous Nanoparticles with Enhanced Biocompatibility. Nanomaterials. 2021;11(4):834.
10. Hameed MF. Impact of TiO_2 Nanoparticles on Physical and Electrical Properties of Mustard Oil for Power Transformer. Institute of Electrical and Electronics Engineers (IEEE); 2022.
11. Palagiri B, Chintaparty R, Nagireddy RR, Imma Reddy VsR. Influence of synthesis conditions on structural, optical and magnetic properties of iron oxide nanoparticles prepared by hydrothermal method. Phase Transitions. 2016;90(6):578-589.
12. Gan YX, Jayatissa AH, Yu Z, Chen X, Li M. Hydrothermal Synthesis of Nanomaterials. Journal of Nanomaterials. 2020;2020:1-3.
13. Hameed HG, Abdulrahman NA. Preparation and Characterization of TiO_2 Nanoparticles With and Without Magnetic Field Effect Via Hydrothermal Technique. Iraqi Journal of Science. 2023:4125-4131.
14. Saif TA, Nadia AA. Cu-ZnO Nanostructures Synthesis and Characterization. Iraqi Journal of Science. 2021:708-717.
15. Arun KJ, Kumar KS, Batra AK, Aggarwal MD, Francis PJJ. Surfactant Free Hydrothermal Synthesis of CdO Nanostructure and Its Characterization. Advanced Science, Engineering and Medicine. 2015;7(9):771-775.
16. Abdulrahman NA. Braggs, Scherre, Williamson–Hall and SSP Analyses to Estimate the Variation of Crystallites Sizes and Lattice Constants for ZnO Nanoparticles Synthesized at different Temperatures. Neuroquantology. 2020;18(1):53-63.
17. Alhumaimess MS, Essawy AA, Kamel MM, Alsohaimi IH, Hassan HMA. Biogenic-Mediated Synthesis of Mesoporous Cu_2O/CuO Nano-Architectures of Superior Catalytic Reductive towards Nitroaromatics. Nanomaterials. 2020;10(4):781.